Satellite Assessments of Regional pCO_2 Distributions and Air-Sea Fluxes of Carbon Dioxide in a River-Dominated Margin

CRUISE REPORT, R/V Pelican Oct. 3-7, 2005

Steven E. Lohrenz
The University of Southern Mississippi, Department of Marine Science

The objective of this cruise was to conduct underway and discrete measurements of pCO_2 and supporting parameters including chlorophyll *a* (chl *a*), suspended particulate matter (SPM), chromophoric dissolved organic matter (CDOM), nutrients, and other measurements in an effort to better understand the mechanisms influencing variations in surface pCO_2 and support effort to develop satellite algorithms to estimate pCO_2 distribution. The multi-disciplinary research approach involves two major activities: 1) *continuous, shipboard, assessments of carbon system properties and air-sea fluxes of CO_2* and relationships to other variables in the river margin shelf ecosystem of the Mississippi River, and 2) t*argeted process measurements* that examine relationships of air-sea carbon flux to net community metabolism, and phytoplankton community composition in different regions of the river-ocean mixing gradient. Process measurements were conducted in at distinct regions along the river-ocean mixing gradient, thereby addressing key natural variability and uncertainties in ocean margin carbon flux.

The cruise track (as shown by the underway salinity map in Figure 1) did not follow a well structured grid as had been originally planned. Weather conditions were characterized by relatively high winds (average 10.5 m s^{-1}) and conditions were too rough to go more than a few miles offshore. After occupying Station 1 outside of Terrebone Bay (Figure 2 and Table 1), the weather conditions and problems with equipment lead to the decision to head east and enter Barataria Bay to anchor overnight. The ship departed Barataria Bay the following morning and proceeded southeast towards the river plume, occupying Stations 3-6. The ship then headed around the eastern edge of the birdfoot delta and into the southern portion of Chandeleur Sound. Conditions were extremely rough at this point with swells in excess of 6 m and no profiling was possible. The ship returned to the river mouth and entered the river on 5 October 2005 and proceeded up to Head of Passes. Station 7 was occupied near Head of Passes and the ship then headed downriver and proceeded out of the mouth and continued southwest occupying Stations 8 and 9 until conditions became too rough to continue, at which point the ship headed northwest in a zig-zag pattern and occupied Stations 10 and 11. At Station 11, a hard drive failure resulted in the loss of the underway pCO_2 data since leaving the river, and it was therefore necessary to return to the river on 6 October. After reaching a stable salinity of around 2, the ship turned downriver and transected in a zigzag to Station 12, and then deadheaded back to Cocodrie to arrive on 7 October.

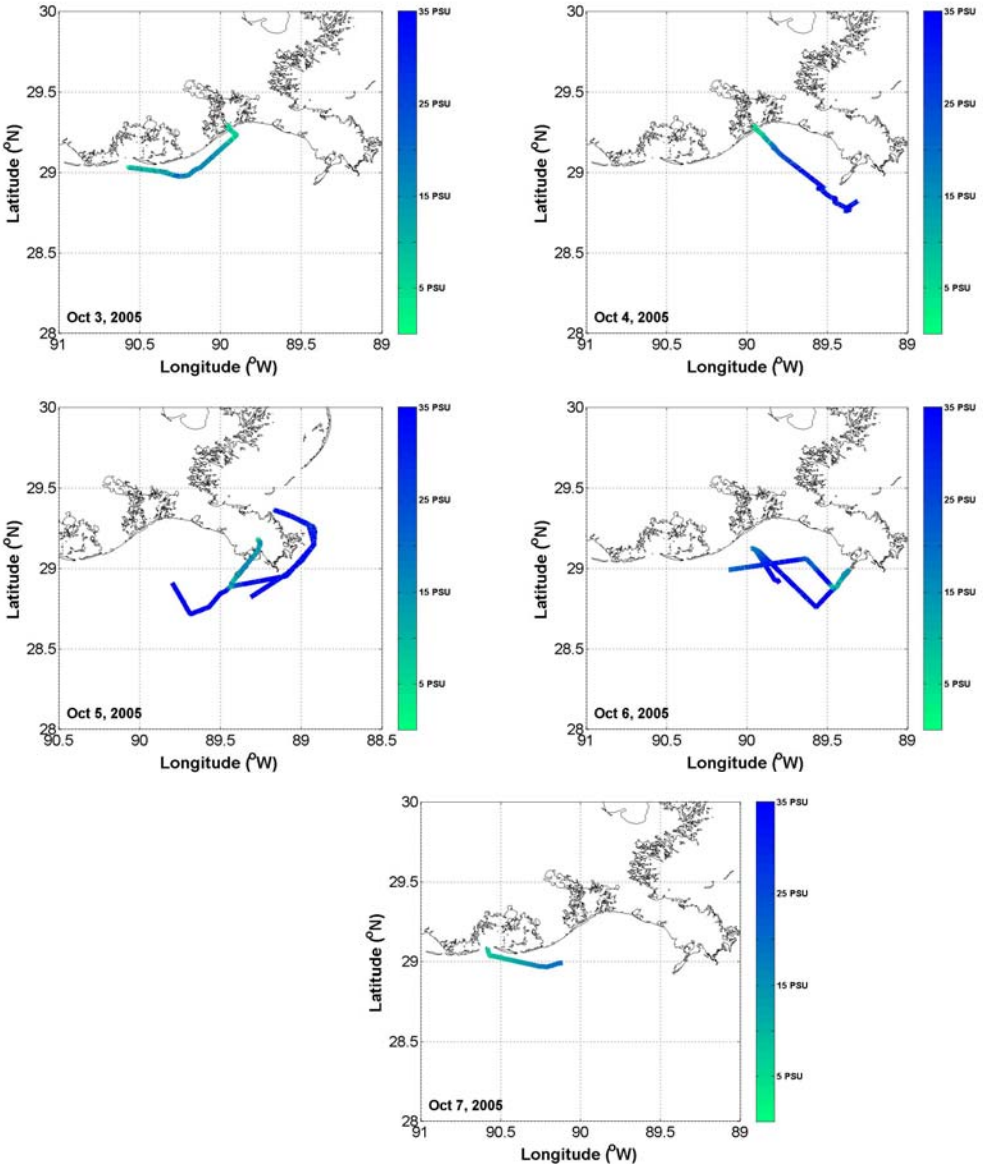

Figure 1 MIDAS tracks on October 3 ~ 7, 2005

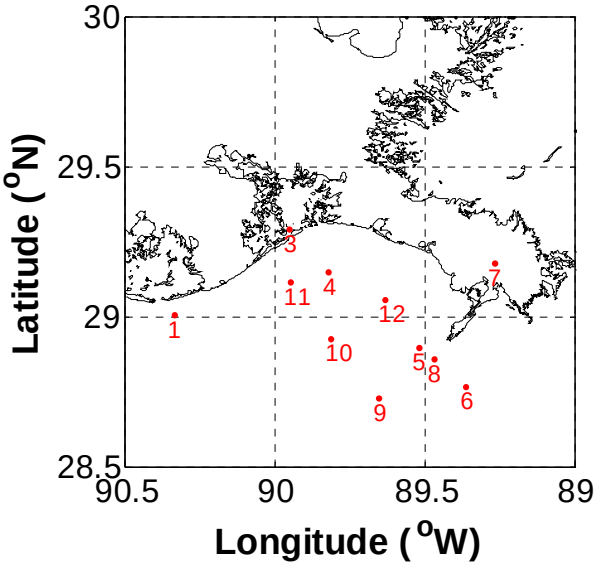

Figure 2. CTD station locations

Vertical profiles were performed with the ship's CTD/Rosette System which was equipped with a Sea-Bird Electronics SBE-9+ Underwater Unit with Digiquartz Pressure Sensor, two temperature sensors (SBE 3-01/F), two conductivity sensors (SBE 4-01/0), pumps (SBE 5-01-3) (2SBE 5T), two dissolved oxygen sensors (SBE 43), transmissometer (Wetlabs CStar 25 cm), fluorometer (Turner SCUFA), sonar altimeter (Benthos PSA-916 altimeter), and Sea-Bird Electronics SBE 32, 12 position Carousel Water Sampler equipped with 5 liter General Oceanics Model 1010 Niskin Bottles.

Surface water was characterized by the ship's flow through MIDAS system, which is a PC based Multiple Instrument Data Acquisition System (MIDAS). The system provides for integration of instrumentation, rapid underway sampling rates, and real-time data display. Analog to digital conversion of sensor signals is performed using using R.M. Young A/D devices with National Instruments LabVIEW controlling software. Navigational data is provided by a Starlink differential GPS or a Trimble GPS with a Micronet Receiver Station. Measurements acquired from a seawater flow-through system include sea surface temperature, conductivity, chlorophyll fluorescence, and transmissometry data using: a Sea-bird Electronics SBE 21 Thermosalinograph; a Sea-Bird Electronics SBE 38 Remote Digital Immersion Thermometer; Turner Designs Model 10 Series Fluorometers; and a WETLabs 10 centimeter or 25.0-centimeter path length transmissometer. Data from the ships meteorological suite is also integrated and sensors include an R.M. Young 05103 Wind Monitor, a R.M. Young model 61201 Barometric Pressure sensor, a R.M. Young TS05327 Temperature and Relative Humidity sensor and a photosynthetically active radiation (PAR) sensor (LI-COR LI-190SZ Quantum Sensor).

Table 1. Sampling time and locations

Station	Zulu Date	Zulu Time	Latitude	Longitude
Station 1	10/3/2005	12:20	29.0043	-90.3331
Station 3	10/4/2005	11:51	29.2907	-89.9500
Station 4	10/4/2005	14:25	29.1485	-89.8198
Station 5	10/4/2005	18:16	28.8982	-89.5186
Station 6	10/4/2005	22:03	28.7671	-89.3615
Station 7	10/5/2005	17:20	29.1774	-89.2662
Station 8	10/5/2005	20:07	28.8580	-89.4696
Station 9	10/5/2005	21:55	28.7287	-89.6516
Station 10	10/6/2005	00:12	28.9274	-89.8119
Station 11	10/6/2005	02:00	29.1143	-89.9477
Station 12	10/6/2005	20:44	29.0582	-89.6319

Measurements

Carbon system measurements

Underway pCO_2 monitoring was carried out using the ship's flow-through system, which was attached to a "shower head equilibrator plus infrared detector (Li7000)" system to measure sea surface pCO_2 with field temperature (Wang and Cai, 2004). Air pCO_2 was measured continuously with another Li7000.

Samples for dissolved inorganic carbon (DIC) and total alkalinity (T_{alk}) taken from Niskin bottles were preserved with $HgCl_2$ and brought back to lab for analysis. Both analyses have a precision of 0.1% and are calibrated using the Certified Reference Material (CRM) from A. G. Dickson (Wang and Cai, 2004).

pH was measured on board with both a spectrophotometric method (Byrne and Breland. 1989) and a Ross Orion glass electrode (Wang and Cai 2004).

Dissolved oxygen (DO) was measured by Winkler titration on board ship on discrete samples with a precision of 0.1-0.2% (a modification of Pai 1993). DO was also measured underway with an Aanderaa DO sensors.

Pigments

Phytoplankton pigments were collected (16 samples from flow-through and 30 samples from CTD stations) by filtration through 47 mm diameter Whatman GF/F filters and storage in liquid nitrogen. HPLC analysis followed the protocol of Wright *et al*. (1991) on a Waters Model 600E Quaternary Gradient HPLC with Model 996 Photodiode Array Detector interfaced with a PC running the Waters Empower2 software in a Window XP operating system environment.

Nutrients and SPM

Inorganic nutrients (NH_3, NO_2/NO_3, PO_4, and Si) were quantified in samples collected from the underway flow-through mapping effort (17 samples), and in discrete samples collected from the CTD/Niskin casts (28 samples). Discrete samples collected on the cruises for inorganic nutrients were analyzed using standard seawater methods and colorometric detection. For SPM, 27 samples (3 samples from flow-through and 24 samples from discrete stations) were filtered onto pre-tared 0.45 μm polycarbonate filters (Poretics), rinsed with isotonic ammonium formate to remove sea salt, and dried until weight is stable.

Dissolved and particulate absorption

Water samples for determining chromophoric dissolved organic matter (CDOM) absorption (12 from flow-through and 23 from CTD stations), particulate pigment and detrital absorption (4 from flow-through and 23 from CTD stations) were collected.

CDOM: Water samples for CDOM were initially filtered through a Whatman 47 mm diameter GF/F filter with a glass filtration apparatus and the filtrate was stored in a dark amber glass bottle with a Teflon-lined cap and refrigerated. Samples were returned to the laboratory and within two weeks, CDOM absorption was determined using a Perkin-Elmer Lamda 2 spectrophotometer with matched 10 cm cylindrical cuvettes with quartz windows. Subsequently, samples were refiltered through a 0.2 μ 47 mm diameter polycarbonate filter and absorption was determined again CDOM absorption was determined in USM's lab by

Quantitative Filter Technique: The quantitative filter pad technique (Lohrenz, 2000 and references therein) was used to determine the particulate pigment and detrital absorption. Samples were filtered onto a Whatman 25 mm GF/F filter and stored in liquid nitrogen until analysis. The optical density of the filter, $OD_f(\lambda)$, was determined with a Perkin Elmer Lambda 18 Spectrophotometer equipped with a Labsphere 150 mm integrating sphere. Filters were placed on a quartz slide at the entrance of the sphere and scanned at a speed of 120 nm min^{-1}. The slit width was 2 nm. Prior to scanning samples, the instrument was zeroed using a blank filter moistened with filtrate. The filter blank measurement, $OD_b(\lambda)$, was also determined. After scanning the sample and blank filters, pigments were extracted from filter pad using a 15 min extraction in hot methanol. The measurement was repeated to obtain the absorption spectrum of the residual particulate detrital material. Correspondingly, a blank filter was also treated with methanol to provide an extracted blank spectrum (Lohrenz, 2000). The OD of the blank filter is subtracted from the sample OD and the baseline of the resulting spectrum is adjusted such that the average OD from 751-800 nm is zero. This adjusted optical density, OD', is converted to absorptance by:

$$A_{fp}(\lambda) = 1 - 10^{-OD'(\lambda)}$$

Finally, the filter pad absorption can be computed by:

$$a_{fp} = \frac{A_{fp}}{\beta\, d_g (1 - A_{fp})}$$

where β is the pathlength amplification factor (a value of 2.76 was recommended by Lohrenz, 2000), and d_g is the geometric pathlength (in meters) given by:

$$d_g = V_f / s$$

where V_f is the volume filtered (in m^3) and s is the clearance area of the filter (in m^2).

The above-mentioned equations are applied to filters and methanol bleached filters to obtain total and detrital absorption respectively. The difference between the two is then pigment absorption.

In-water optics

Water column absorption and attenuation were measured using WET Labs, Inc. ac-9 and ac-s meters. The instruments were mounted together on a frame with a SeaBird SBE25 Sealogger CTD to provide vertical profile information. The details of data correction are described in Appendix.

Vertical profiles of subsurface upwelling radiance and downwelling irradiance were determined using a MicroPro II (Satlantic, Inc.), a free-fall multispectral profiling radiometer that measures at 400, 412, 443, 456, 490, 510, 532, 555, 565, 620, 665, 683, 705, and 780 nm. The data was processed using ProSoft v7.7.8 (Satlantic, Inc.).

Above water radiometry

Above-water total upwelling radiance (L_t), sky radiance (L_s), and downwelling irradiance (E_d) were acquired with a HyperSAS-UV optical remote sensing system (Satlantic, Inc.), The system was comprised of two 166-channel MiniSpec radiance sensors and one 166-channel MiniSpec irradiance sensor for measurements in both UV (350-400 nm) and visible (400-800 nm) wavelengths. Additionally integrated into the optical system are discrete sensors at selected UV wavelengths (305, 325, 340, 380 nm) and one red wavelength (671 nm). A pitch and roll sensor was also incorporated into the data stream to provide complementary orientation information. An integrated Garmin GPS provided position, as well as ship's heading and speed.

The HyperSAS-UV was mounted on the crow's nest at a height of approximately 9 m. Zenith and nadir viewing angles of the radiance sensors were 45^o. The orientation of the sensors relative to the sun's plane was considered in the evaluation of the data. Relative solar azimuthal angles of 90^o-135^o were considered preferable (Hooker et al., 2004). Data were discarded in situations where conditions were unsuitable for collection.

Remote sensing reflectance (R_{rs}, sr^{-1}) was estimated according to Mobley (1999) using the following formula:

$$R_{rs}(\theta,\phi,\lambda) = \frac{L_w(\theta,\phi,\lambda)}{E_d(\lambda)}$$

where θ and ϕ represent the polar and azimuthal directions, λ is wavelength, and L_w is water leaving radiance. L_w is estimated as:

$$L_w(\theta,\phi,\lambda) = L_t(\theta,\phi,\lambda) - \rho L_s(\theta',\phi',\lambda)$$

where θ' and ϕ' represent the skyward directions from which radiance would be specularly reflected into directions θ and ϕ (Mobley, 1999). A constant value of ρ=0.028 was assumed unless otherwise indicated (*cf.* Mobley, 1999).

Data were filtered to remove effects of episodic sun glint as well as more periodic variations associated with sky glint (Hooker, et al., 2002; Hooker and Morel, 2003) and sea foam from the ship's wake. Filtering was accomplished by eliminating all spectra with the exception of those having the lowest 5% of values in the near infrared (~780 nm). A final step applied as necessary to reduce outliers was to eliminate spectra for which values in the near infrared (~780 nm) fell outside the range of 50% of one standard deviation from the mean. Additional baseline corrections were applied in some cases by subtracting the value of R_{rs} at 780 nm from values for all wavelengths for a given HyperSAS spectrum. For the discrete UV measurements, baseline corrections were made by subtracting the minimum value of the discrete UV R_{rs} measurements from all discrete UV measurements for a given spectrum.

Primary production

At three stations (Stations 5, 8, and 12, five depths total) photosynthesis-irradiance (P-E) parameters were determined by incubation with $^{14}C\text{-}HCO_3^-$ as described in Lohrenz *et al*. (1994).

Participants

The participants of this cruise include Steven Lohrenz (USM, Chief Scientist), Feizhou Chen (UGA), Justin Hartmann (UGA), Merritt Tuel (USM), Xiaogang Chen (USM), Jessica Lacy (USM), Egan Rowe (USM), and Courtney Stringer (USM).

Reference

Lohrenz, S. E., G. L. Fahnenstiel, D. G. Redalje (1994). Spatial and temporal variations of photosynthetic parameters in relation to environmental conditions in coastal waters of the Northern Gulf of Mexico. Estuaries 17(4): 779-795.

Lohrenz, S. E. (2000). A novel theoretical approach to correct for pathlength amplification and variable sampling loading in measurements of particulate spectral absorption by the quantitative filter technique. Journal of Plankton Research 22(4): 639-657.

Pai, S. C. (1993). Determination of dissolved oxygen in seawater by direct spectrophotometry of total iodine. Mar. Chem. 41: 343.

Wang, Z. H. A. and W. J. Cai (2004). Carbon dioxide degassing and inorganic carbon export from a marsh-dominated estuary (the Duplin River): A marsh CO_2 pump. Limnol. Oceanogr. 49(2): 341-354.

Wright, S. W., S. W. Jeffrey, R. F. C. Mantoura, C. A. Llewellyn, T. Bjornland, D. Repeta and N. Welschmeyer (1991). Improved HPLC method for the analysis of chlorophylls and carotenoids from marine phytoplankton. Mar. Ecol. Prog. Ser. 77: 183-196.

Appendix: a/c Meters Data Corrections

The thermal and water calibration corrections of *a/c* is performed as:

$$a_{T\ corr}(\lambda) = a_{measured}(\lambda) - \Psi_T(T_w - 25) - (a_w(\lambda) - \Psi_T(T_{cal} - 25))$$

$$c_{T\ corr}(\lambda) = c_{measured}(\lambda) - \Psi_T(T_w - 25) - (c_w(\lambda) - \Psi_T(T_{cal} - 25))$$

where T_w and T_{cal} are the water temperature during sampling and calibration respectively. $a_w(\lambda)$ is the clean water calibration value. Ψ_T is given (Pegau *et al.*, 1997) by:

$$\Psi_T = \sum \{ M_T\ (M/\sigma) \exp - [\ (\lambda - \lambda_c)^2 / 2\sigma^2\ ] \}$$

The magnitude, M, width, σ, central wavelength, λ_c, and temperature percentage multiplier, M_T (Table 2) are taken from Table 3 of Pegau *et al.* (1997).

The scattering correction (Zaneveld *et al*., 1994) is also applied to the unfiltered *a* measurements:

$$a_{scatter\ corr}(\lambda) = a_{T\ corr}(\lambda) - [\ c_{T\ corr}(\lambda) - a_{T\ corr}(\lambda)\ ) * \{\ a_{T\ corr}(715) / (c_{T\ corr}(715) - a_{T\ corr}(715)\ \}\ ]$$

Finally, the absorption and attenuation of pure water at each wavelength will be added. The values for pure ware *a* and *c* at each wavelength are compiled from the published values of Sogandares and Fry (1997), Pope and Fry (1997), and Buiteveld *et al.* (1994). (Table 3, 4)

Table 2. Values of M, σ, λ_c, and M_T (Table 3 of Pegau *et al.,* 1997)

M	σ	λ_c	M_T
0.18	18	453	0.0045
0.17	15	485	0.002
0.52	14	517	0.0045
1.4	20	558	0.002
4.6	17.5	610	0.0045
2.1	15	638	-0.004
4.3	17	661	0.002
9.6	22	697	-0.001
1.6	6	740	0.0045
34	18	744	0.0062
18	20	775	-0.001
42	25	795	-0.001

Table 3. Pure water absorption, taken from: Sogandares and Fry (1997) and Pope and Fry (1997).

λ	a (m^{-1})	λ	a (m^{-1})	λ	a (m^{-1})	λ	a (m^{-1})
340	0.0325	505	0.0256	632.5	0.2995	752	2.7413
350	0.0204	507.5	0.028	635	0.3012	754	2.7478
360	0.0156	510	0.0325	637.5	0.3077	756	2.7542
370	0.0114	512.5	0.0372	640	0.3108	758	2.7628
380	0.01	515	0.0396	642.5	0.322	760	2.771
390	0.088	517.5	0.0399	645	0.325		
392.5	0.00829	520	0.0409	647.5	0.335		
395	0.00813	522.5	0.0416	650	0.34		
397.5	0.00775	525	0.0417	652.5	0.358		
400	0.00663	527.5	0.0428	655	0.371		
402.5	0.00579	530	0.0434	657.5	0.393		
405	0.0053	532.5	0.0447	660	0.41		
407.5	0.00503	535	0.0452	662.5	0.424		
410	0.00473	537.5	0.0466	665	0.429		
412.5	0.00452	540	0.0474	667.5	0.436		
415	0.00444	542.5	0.0489	670	0.439		
417.5	0.00442	545	0.0511	672.5	0.448		
420	0.00454	547.5	0.0537	675	0.448		
422.5	0.00474	550	0.0565	677.5	0.461		
425	0.00478	552.5	0.0593	680	0.465		
427.5	0.00482	555	0.0596	682.5	0.478		
430	0.00495	557.5	0.0606	685	0.486		
432.5	0.00504	560	0.0619	687.5	0.502		
435	0.0053	562.5	0.064	690	0.516		
437.5	0.0058	565	0.0642	692.5	0.538		
440	0.00635	567.5	0.0672	695	0.559		
442.5	0.00696	570	0.0695	697.5	0.592		
445	0.00751	572.5	0.0733	700	0.624		
447.5	0.0083	575	0.0772	702.5	0.663		
450	0.00922	577.5	0.0836	705	0.704		
452.5	0.00969	580	0.0896	707.5	0.756		
455	0.00962	582.5	0.0989	710	0.827		
457.5	0.00957	585	0.11	712.5	0.914		
460	0.00979	587.5	0.122	715	1.007		
462.5	0.01005	590	0.1351	717.5	1.119		
465	0.01011	592.5	0.1516	720	1.231		
467.5	0.0102	595	0.1672	722.5	1.356		
470	0.0106	597.5	0.1925	725	1.489		
472.5	0.0109	600	0.2224	727.5	1.678		
475	0.0114	602.5	0.247	728	1.487		
477.5	0.0121	605	0.2577	730	1.6211		
480	0.0127	607.5	0.2629	732	1.7872		
482.5	0.0131	610	0.2644	734	1.9917		
485	0.0136	612.5	0.2665	736	2.2074		
487.5	0.0144	615	0.2678	738	2.3942		
490	0.015	617.5	0.2707	740	2.5319		
492.5	0.0162	620	0.2755	742	2.6231		
495	0.0173	622.5	0.281	744	2.6723		
497.5	0.0191	625	0.2834	746	2.7021		
500	0.0204	627.5	0.2904	748	2.7216		
502.5	0.0228	630	0.2916	750	2.7334		

Table 4. Pure water scattering coefficient taken from: H. Buiteveld *et al*. (1994, Table 1)

λ	b (m^{-1})	λ	b (m^{-1})	λ	b (m^{-1})	λ	b (m^{-1})	λ	b (m^{-1})
340	0.0104	440	0.0036	540	0.0015	640	0.0008	740	0.0004
342	0.0101	442	0.0035	542	0.0015	642	0.0007	742	0.0004
344	0.0099	444	0.0034	544	0.0015	644	0.0007	744	0.0004
346	0.0096	446	0.0034	546	0.0015	646	0.0007	746	0.0004
348	0.0094	448	0.0033	548	0.0014	648	0.0007	748	0.0004
350	0.0092	450	0.0033	550	0.0014	650	0.0007	750	0.0004
352	0.009	452	0.0032	552	0.0014	652	0.0007	752	0.0004
354	0.0088	454	0.0031	554	0.0014	654	0.0007	754	0.0004
356	0.0086	456	0.0031	556	0.0014	656	0.0007	756	0.0004
358	0.0084	458	0.003	558	0.0013	658	0.0007	758	0.0004
360	0.0082	460	0.003	560	0.0013	660	0.0007	760	0.0004
362	0.008	462	0.0029	562	0.0013	662	0.0007		
364	0.0078	464	0.0029	564	0.0013	664	0.0006		
366	0.0076	466	0.0028	566	0.0013	666	0.0006		
368	0.0075	468	0.0028	568	0.0012	668	0.0006		
370	0.0073	470	0.0027	570	0.0012	670	0.0006		
372	0.0071	472	0.0027	572	0.0012	672	0.0006		
374	0.007	474	0.0026	574	0.0012	674	0.0006		
376	0.0068	476	0.0026	576	0.0012	676	0.0006		
378	0.0067	478	0.0025	578	0.0012	678	0.0006		
380	0.0065	480	0.0025	580	0.0011	680	0.0006		
382	0.0064	482	0.0024	582	0.0011	682	0.0006		
384	0.0063	484	0.0024	584	0.0011	684	0.0006		
386	0.0061	486	0.0024	586	0.0011	686	0.0006		
388	0.006	488	0.0023	588	0.0011	688	0.0006		
390	0.0059	490	0.0023	590	0.0011	690	0.0006		
392	0.0058	492	0.0022	592	0.001	692	0.0005		
394	0.0056	494	0.0022	594	0.001	694	0.0005		
396	0.0055	496	0.0022	596	0.001	696	0.0005		
398	0.0054	498	0.0021	598	0.001	698	0.0005		
400	0.0053	500	0.0021	600	0.001	700	0.0005		
402	0.0052	502	0.0021	602	0.001	702	0.0005		
404	0.0051	504	0.002	604	0.001	704	0.0005		
406	0.005	506	0.002	606	0.0009	706	0.0005		
408	0.0049	508	0.002	608	0.0009	708	0.0005		
410	0.0048	510	0.0019	610	0.0009	710	0.0005		
412	0.0047	512	0.0019	612	0.0009	712	0.0005		
414	0.0046	514	0.0019	614	0.0009	714	0.0005		
416	0.0045	516	0.0018	616	0.0009	716	0.0005		
418	0.0044	518	0.0018	618	0.0009	718	0.0005		
420	0.0043	520	0.0018	620	0.0009	720	0.0005		
422	0.0042	522	0.0018	622	0.0009	722	0.0005		
424	0.0042	524	0.0017	624	0.0008	724	0.0005		
426	0.0041	526	0.0017	626	0.0008	726	0.0004		
428	0.004	528	0.0017	628	0.0008	728	0.0004		
430	0.0039	530	0.0017	630	0.0008	730	0.0004		
432	0.0038	532	0.0016	632	0.0008	732	0.0004		
434	0.0038	534	0.0016	634	0.0008	734	0.0004		
436	0.0037	536	0.0016	636	0.0008	736	0.0004		
438	0.0036	538	0.0016	638	0.0008	738	0.0004		

References

Buiteveld, H., J. H. H. Hakvoort, and M. Donze (1994) The optical properties of pure water, in Ocean Optics XII, J.S.Jaffe, ed., Proc SPIE 2258: 174-183.

Pegau, W. S., D. Gary, and J. R. V. Zaneveld (1997) Absorption and attenuation of visible and near-infrared light in the water: dependence on temperature and salinity. Appl. Opt. 36(24): 6035-6046.

Pope, R. M. and E. S. Fry (1997) Absorption spectrum (380-700nm) of pure water. II. Integrating cavity measurements. Appl. Opt., 36(33): 8710-8723.

Sogandares, F. M. and E. S. Fry (1997) Absorption spectrum (340-640nm) of pure water. I. Photothermal measurements. Appl. Opt., 36(33): 8699-8709.

Zaneveld, J.R.V., J. C. Kitchen and C. C. Moore (1994) Scattering error correction of reflecting tube absorption meter, Ocean Optics XII, Proc. Soc. Photo-Optical Instrum. Eng. (SPIE), Vol. 2258, 44–55.